Clim. Past Discuss., https://doi.org/10.5194/cp-2017-77
Manuscript under review for journal Clim. Past
Discussion started: 7 July 2017

Climate of the Past Discussions

Strengthening of the Somali upwelling during the Holocene and its impact on southwest monsoon rainfall

Balaji D.[1,2], Ravi Bhushan[2], L. S. Chamyal[1]

[1]Department of Geology, The Maharaja Sayajirao University of Baroda, India
[2]Geoscience Division, Physical Research Laboratory, Ahmedabad, India

Correspondence to: Balaji D. (balaji.d86@gmail.com)

Abstract. The history of the Somali upwelling during the last 18.5 ka has been reconstructed using biogenic silica fluxes estimated from a sediment core retrieved from the western Arabian Sea. The reconstructed record demonstrates periodic weakening and strengthening of the Somali upwelling during the past 18.5 ka. Variations in biogenic silica fluxes suggest weak upwelling during the last glacial period (18.5-15 ka BP). Strengthened upwelling during the Bølling-Allerød period (15-13 ka BP) points to post-glacial onset of the southwest monsoon. The Younger Dryas (13-11 ka BP) is again marked by reduced upwelling strength. Intensification of the Somali upwelling at the beginning of the Holocene and a decline at 8 ka BP are observed. Increases in upwelling strength recorded since 8 ka BP suggest strengthening of the southwest monsoon during the latter part of the Holocene. Linking these upwelling variations with southwest monsoon precipitation, a major shift in the relationship between the strength of the Somali upwelling and southwest monsoon rainfall from positive to negative has occurred during the pre-Holocene to the Holocene. The observed shift is attributed to the variation in the southwest monsoon strength due to the latitudinal shift of the Intertropical Convergence Zone (ITCZ) associated with changes in moisture sources.

1 Introduction

The greater part of the world's population inhabits the tropical region, where climate is mainly controlled by monsoon rainfall. Understanding the causes of past changes thus plays a critical role in deciphering past, present and future monsoon variability. The economy of India, which is a tropical country that contains a significant part of the world's population, is dependent to a large extent on the southwest monsoon (SWM) rainfall; hence, slight changes in SWM rainfall can lead to immense societal impacts. Several attempts have been made to identify the factors responsible for SWM rainfall variations. SWM rainfall variability is correlated with several global phenomena, such as ENSO (Goswami et al., 1999; Annamalai and Liu, 2005), Atlantic SST (Goswami et al., 2006; Yadav, 2016), Eurasian snow cover (Hahn and Shukla, 1976; Pant and Rupa Kumar, 1997; Bamzai and Shukla, 1999), the pre-monsoon 500 hPa ridge (Mooley et al., 1986), the Indo-Pacific warm pool (Parthasarathy et al., 1988; Parthasarathy et al., 1991), the Pacific decadal oscillation (Krishnan and Sugi, 2003), and the Atlantic multi-decadal oscillation (Krishnamurthy and Krishnamurthy, 2015). In addition to these factors that influence SWM, the Indian Ocean Warm Pool (IOWP) has been identified as the prominent source of moisture for SWM rainfall (Ninomiya

Clim. Past Discuss., https://doi.org/10.5194/cp-2017-77
Manuscript under review for journal Clim. Past
Discussion started: 7 July 2017

and Kobayashi, 1999). During its maxima, the IOWP extends throughout the northern Indian Ocean during the pre-monsoon period (April), and it almost reduces to half during the SWM (Izumo et al., 2008). The extent of the IOWP is primarily affected by the Somali upwelling and partly by the latent heat flux increase in the Arabian Sea during the SWM season (Izumo et al., 2008). The Somali upwelling, as well as SWM rainfall, are caused by the SWM winds during boreal summer.

Upwelling of deep water during the SWM brings nutrients up to the photic zone, enhancing surface productivity in the western Arabian Sea. Paleoproductivity variations in the coastal regions off Somalia and Oman have been extensively studied to understand past changes in SWM-related upwelling (Sirocko et al., 1993; Naidu and Malmgren, 1996; Gupta et al., 2003; Tiwari et al., 2010). However, variations in siliceous productivity in the western Arabian Sea, which have direct implications for the strength of upwelling in the past, have not been understood. The present study thus aims to understand past variations in siliceous productivity in the Somali upwelling region, as well as paleo-upwelling strength and its relationship with the southwest monsoon rainfall, using a sediment core retrieved from the western Arabian Sea (Fig.1).

1.1 Modern Oceanography and Productivity

The surface water circulation in western Arabian Sea is controlled by seasonal changes in atmospheric wind pattern related with annual migration of ITCZ (Wyrtki, 1973). During boreal winter, ITCZ stays south of equator and shifts to north during boreal summer. This northward shift of ITCZ during southwest monsoon (SWM, June-September) season drives the southern hemisphere eastern trade winds across equator that turns clockwise and becomes southwest winds (Findlater, 1977; Fig. 2). These southwest winds help to form the Somali current along the east African coast towards north. The Somali current is generally associated with near shore upwelling and eddies such as southern gyre, great whirl and Soccotra eddy (Schott et al., 1990; Beal and Chereskin, 2003; Schott et al., 2009). These eddies induce intense upwelling which pumps out the low temperature and nutrient rich subsurface water to the surface along the east coast of Africa (Young and Kindle, 1994).

Productivity in western Arabian Sea reflects the seasonal changes in surface ocean characteristics (Qasim, 1977; Brock et al., 1991). More than half of the annual productivity in the western Arabian Sea occurs during southwest monsoon due to intense upwelling (Haake et al., 1993). Total flux (biogenic + dust) also peaks at the same time when productivity is at its maximum, means SWM not only cause high productivity in the western Arabian Sea but also high dust flux (Sirocko and Lange, 1991; Haake et al., 1993). Sediment trap studies in western Arabian Sea recorded that during the onset of SWM, biogenic carbonate dominates particle flux, while the end of SWM is dominated by biogenic silica flux (Konning et al., 2001). This late SWM appearance of biogenic silica flux is caused by the increased surface silicate concentration of upwelled deep water. Initially, this upwelled deep waters surfaced at Somali coastal upwelling zone and transported towards the mouth of Gulf of Aden (core location) through the Socotra channel i.e. between the Socotra Island and Somalia (Young and Kindle, 1994).

Clim. Past Discuss., https://doi.org/10.5194/cp-2017-77
Manuscript under review for journal Clim. Past
Discussion started: 7 July 2017

Climate of the Past Discussions
Open Access
EGU

2 Material and methods

Sediment core SS4018 was collected off the Horn of Africa (north of Socotra island), in the western Arabian Sea (13° 12.80' N, 53° 15.40' E; water depth 2830 m; core length 130 cm; Fig. 1) during FORV Sagar Sampada cruise SS-164 in 1998. Sub-sampling at 2-cm intervals was carried out. The age-depth model Fig. 3) as well as the calcareous and organic productivity proxies of this sediment core have been presented elsewhere (Tiwari et al., 2010). Dry bulk density (DBD) was computed using an empirical equation based on the calcium carbonate concentrations (Clemens et al., 1987). The flux rate was estimated using an average sedimentation rate computed based on the age-depth model given by Tiwari et al., (2010). However, the published ages of the individual samples were considered. The sedimentation rate at the core site as given by Tiwari et al., (2010) is variable, the lowest being 3.5 and highest 22.7 cm.ka-1. Since the age model depends on the sample selection criteria and may change according to depth of age control points, an average sedimentation rate was computed for the entire core.

The biogenic silica concentration was measured in each sample using the method described by Carter and Colman (1994). Dried homogenized samples weighing 50 mg were placed in centrifuge tubes. Five milliliters of 10 % H2O2 was added to each sample at room temperature, and the samples were stored for 2 hours to remove organic matter. Five milliliters of 1N HCl was added to each tube. After acid treatment, 20 ml of distilled water was added, and the samples were centrifuged for 15 minutes. Sample tubes were kept in an oven after removal of the supernatant. Thirty milliliters of 2 M Na2CO3 was added to each sample tube, and the tubes were kept in a shaker bath at 95^0 C for 5 hours. After 5 hours, the samples were centrifuged for 5 minutes, and 3 ml of hot supernatant was pipetted out of each sample and added to exactly 30 ml of distilled water in pre-cleaned sample tubes. These solutions were acidified by adding 0.9 ml of concentrated HNO3. Sample tubes were sealed after effervescence. Silicon and aluminum concentrations were measured in these samples using ICP-AES (Jobin-Yuvon, Model 38S at Physical Research Laboratory, Ahmedabad). The silicon concentrations were then corrected for clay mineral dissolution by using the formula given by Carter and Colman (1994) (Eqn 1):

$$\Delta Si = Si - (Al * 1.93) \quad (1)$$

Where, ΔSi is the corrected silicon concentration, Si and Al are the measured concentrations of silicon and aluminium in the sample, and 1.93 is the Si to Al ratio in smectite. Smectite is an abundant clay mineral in the northern Arabian Sea (Sirocko et al., 1991). Biogenic silica concentrations were calculated using the formula given below (Eqn 2):

$$Biogenic\ silica = \Delta Si * \mathcal{K} \quad (2)$$

Where, K is a constant that equals 2.4, which accounts for the ~10 % water content in biogenic silica (Mortlock and Frolich, 1989). Overall, the error associated with the biogenic silica measurement is less than 5 % based on repeat measurements. The biogenic silica flux is calculated by multiplying the biogenic silica fraction by the sedimentation rate (SR) and the dry bulk density (DBD) (Eqn 3),

$$B.Si.flux(g.m^{-2}.y^{-1}) = B.Si * SR(m.y^{-1}) * DBD(g.m^{-3}) \quad (3)$$

The uncertainties associated with the biogenic silica concentration (B.Si) is estimated from the error in Aluminium and Silicon concentration based on measurements of repeat and standard material. The maximum error in biogenic silica concentration is

Clim. Past Discuss., https://doi.org/10.5194/cp-2017-77
Manuscript under review for journal Clim. Past
Discussion started: 7 July 2017

Climate of the Past Discussions

within 5%. Dry bulk density (DBD) is calculated from CaCO3 concentration using an empirical equation suggested by Clemens et al., 1987. The standard uncertainty in DBD calculation is 0.091 g/cm3. The uncertainty in average sedimentation rate (SR) is 0.12 cm/ky. Finally the uncertainty associated with biogenic silica flux (B.Si flux) is propagated using the below equation,

$$\sigma B.Si\ flux = B.Si\ flux * \sqrt{\{(\sigma B.Si/_{B.Si})^2 + (\sigma DBD/_{DBD})^2 + (\sigma SR/_{SR})^2\}} \quad (4)$$

Where, prefix "σ" stands for uncertainty. Uncertainty in biogenic silica concentration is below 5%. But the uncertainty in flux are up to 15%. This increase in uncertainty is due to the high standard error associated with empirical derivation of Dry bulk density.

3 Results

Biogenic silica concentrations varied from 3 % to 15.2 % during the last 18.5 ka (Table 1), with the lowest concentrations (3–4 %) being observed at the bottom of the core between 18.5 ka and 16 ka BP. Subsequently, it increased continuously up to 13.5 ka BP (~9 %) and decreased to 6.5 % at ~13 ka BP. No significant variations in biogenic silica concentration s were observed between 13 ka and 11.3 ka BP. After 11.3 ka BP, biogenic silica increased from 6.5 % to 10.5 % and remained stable for a period of almost 1000 years until 10 ka BP. The biogenic silica concentration increased from 10.5 % to 12 % during 10–9.5 ka BP, and it decreased subsequently to 8.5 % at 8 ka BP. From 8 ka to 7.3 ka BP, it changed from 8.5 % to 9.5 % with a peak at 7.7 ka BP (13.3 %), then it remained stable until 6 ka BP. From 6 ka to 5 ka BP, the biogenic silica concentration increased from 10 % to 12.5 % and then decreased at 4 ka BP. After 4 ka BP, a continuous increase to a maximum value of 15 % biogenic silica at 1.5 ka BP and a subsequent decrease to 12 % at 1 ka BP were observed. Biogenic silica concentrations showed no variations during the last 1 ka BP.

The variations in biogenic silica fluxes show an overall increasing trend from 18.5 ka to present (Fig.4). The fluxes varied between 1.4 to 6.8 g.m-2.y-1. The minimum values (<2 g.m-2.y-1) occur at the bottom of the sediment core, i.e., between 18.5and 16 ka BP, and the maximum flux value is observed at 2 ka BP. Five distinct peaks in biogenic silica flux during the last 18.5 ka BP were observed between 14–13 ka, 11–10 ka, 10–9 ka, 6–4 ka and 2.5–1 ka BP. Uncertainties in biogenic silica concentrations and fluxes are below 5 % and up to 15 %, respectively. The increase in uncertainty in the flux is due to the high standard error associated with the empirical derivation of the dry bulk densities.

4 Discussion

4.1 Biogenic silica flux as an upwelling proxy

The surface waters of the world ocean are mostly deficient in bioavailable silica (Hurd, 1973), which is a major nutrient for siliceous productivity. Apart from the Southern Ocean, high siliceous productivity can be observed in the major upwelling regions, where upwelled nutrient-rich water causes high primary production (Koning et al., 2001). The ocean is under saturated

Clim. Past Discuss., https://doi.org/10.5194/cp-2017-77
Manuscript under review for journal Clim. Past
Discussion started: 7 July 2017

with respect to silica, and thus biogenic silica flux preservation in sediments is a function of its export flux, which is controlled by its dissolution both in the water column and at the sediment water interface (Hurd, 1989; Broecker and Peng, 1982). Thus, using biogenic silica as a proxy for the study of paleo-upwelling requires understanding of its burial efficiency. Studies of sediment trap data and surface sediments (Koning et al., 1997; Koning et al., 2001) of the Somali basin provides better estimates of the burial efficiency of biogenic silica in the western Arabian Sea. Only 6.8–8.7 % of diatom (biogenic silica) productivity is preserved in the sediments of the Somali basin; the rest is dissolved in the water column as well as at the sediment water interface (Koning et al., 2001). One of the major findings from sediment traps in the Somali basin by Koning et al., (2001) is the selective preservation of upwelling-indicating diatoms in the sediments of the Somali region. This is linked to the silicification of diatom frustules; most pre- and post-upwelling produced diatoms are weakly silicified, enhancing their dissolution in the water column and leading to their low preservation in sediments. Despite attributing the lowest preservation efficiency to the low biogenic silica fluxes observed at the bottom of the core and the highest preservation efficiency to the high biogenic silica fluxes at the top, the variation is still approximately three times greater. Hence, the influence of preservation efficiency on our core record is minimal.

Apart from biogenic silica production and preservation efficiency, sediment redistribution can also influence the biogenic silica flux. However, considering the sediment core location and average sedimentation rate, it is likely that the influence of sediment focusing/winnowing on the flux record is minimal. The location of the sediment core is far from the continental slope (Fig. 1) and not directly influenced by coastal currents or fluvial systems that would lead to redistribution of the sediment flux. The chronology of the sediment record is based on the published age-model given by Tiwari et al., (2010). The model, however, shows sizeable variations in the sedimentation rate. Because the calculated sedimentation rate is a function of the selected sampling depths (which may vary), the average rate of sedimentation has been considered in estimating the fluxes of biogenic silica. The high surface production of biogenic silica during SWM upwelling (Haake et al., 1993; Koning et al., 1997), together with the increased burial efficiency of upwelling-indicating diatoms (biogenic silica) in the western Arabian Sea sediments (Koning et al., 2001), makes biogenic silica flux as a potential proxy for SWM-related upwelling in the study area. To validate this we have compared the SST records (Huguet et al., 2006; Saher et al., 2007; Anand et al., 2008) from the Somali upwelling region with our biogenic silica flux record (Fig. 5). Synchronous but opposite (upwelling induce high biogenic silica flux and low SST) changes in biogenic silica flux and SST indicates the potential of biogenic silica flux as important proxy for upwelling in our study area.

4.2 Somali upwelling strength versus southwest monsoon rainfall

Western Arabian Sea surface temperatures during SWM are directly related to upwelling strength (enhanced upwelling results in lower SSTs and vice versa). Vecchi and Harrison (2004) observed a strong positive correlation between western Arabian SSTs and SWM rainfall over the Western Ghats Mountains in India from 1982 to 2001. An observational and modelling study by Izumo et al., (2008) indicates the causes for the variations in western Arabian Sea SSTs and their influence on SWM rainfall over the Western Ghats. According to Izumo, increased Somali upwelling during the SWM reduces the westward extension

Clim. Past Discuss., https://doi.org/10.5194/cp-2017-77
Manuscript under review for journal Clim. Past
Discussion started: 7 July 2017

of the IOWP during summer, which decreases moisture availability to the air mass that delivers rainfall to the western part of the Indian sub-continent.

Did this anti-correlation exist between the Somali upwelling and SWM rainfall in the geological past? To answer this question, we need to investigate the record of paleo-upwelling in the Somali region and paleo-rainfall in the western part of India and adjoining areas. There are no terrestrial records of paleo-rainfall covering the last 18.5 ka from the Western Ghats, but there are several paleoclimatic records based on marine sediment cores from the eastern Arabian Sea. The biogenic silica flux temporal variability is compared with paleo-rainfall records ($\delta^{18}O_w$ of surface water (Anand et al., 2008), surface water salinity (Govil and Naidu, 2010)) from the eastern Arabian Sea and a speleothem record from Oman (Fleitmann et al., 2007; Fig. 6). Since the records are from different regions and have irregular temporal resolutions, we only examine the long-term trends.

4.2.1 Last Glacial Period (18.5–15 ka BP)

The biogenic silica flux record does not show any distinct variation between the previously identified Heinrich event 1 and the Last Glacial Maximum (LGM). So the period between 18.5 and 15 ka is considered here as the Last Glacial Period (LGP). Both biogenic silica concentrations (3–5 %) and fluxes (~2 g.m-2.y-1) were lowest during the LGP (Fig. 4), which is similar to earlier findings of low productivity during glacial periods from the western Arabian Sea (Burckle, 1989; Sirocko et al., 1991; Sirocko et al., 2000; Ivanochko et al., 2005; Tiwari et al., 2010). Based on the modern pattern of biogenic silica productivity and its burial efficiency in the western Arabian Sea, the observed low fluxes of biogenic silica indicate that the Somali upwelling was very weak during the LGP. However, the lowest SSTs in the last 18.5 ka were recorded in the Somali basin during the LGP (Huguet et al., 2006; Saher et al., 2007; Anand et al., 2008), is contrary to our interpretation (Fig. 5). These low SSTs in the Somali basin might have been caused by a basin-wide reduction in SST by at least 2–4° C during the LGP (Dahl and Oppo, 2006), rather than by the SWM upwelling. Thus, the formation of the IOWP (SST>28° C) during the LGP can be ruled out. Weakened SWM rainfall during the LGP has also been envisaged by Anand et al. (2008) based on high $\delta^{18}O$ in sediment core off Goa, while Govil and Naidu. (2010) observed evidence of high salinities in a sediment record from off Goa that was attributed to high evaporation and low fresh water influx. Based on the weak upwelling in the western Arabian Sea and the increase in evaporation and reduced fresh water influx to the eastern Arabian Sea, it is concluded that the SWM was weak during the LGP.

4.2.2 Deglacial Period (15–11 ka BP)

The Deglacial Period (DP) is a connecting phase between two entirely different climatic periods, the LGP and the Holocene. The DP is actually a composite of two bi-millennial scale events between 15–13 ka and 13–11 ka BP. The period occupied by these two events nearly coincides with well-known climatic phases, specifically the Bølling-Allerød (B/A) period and the Younger Dryas (YD) event. The beginning of the B/A is marked by an abrupt increase in biogenic silica flux (Fig. 5a), which we attribute to the effect of entrainment of the SWM at our core site and the subsequent increase in Somali upwelling strength. This is further supported by investigation of Zr/Hf in two independent sediment cores near our core site, which shows an

Clim. Past Discuss., https://doi.org/10.5194/cp-2017-77
Manuscript under review for journal Clim. Past
Discussion started: 7 July 2017

increasing flux of windborne dust from the Horn of Africa (an indicator of the SWM) at the onset of the B/A (Sirocko et al., 2000; Isaji et al., 2015). The reduction in SSTs during the B/A in the Somali basin (Huguet et al., 2006; Saher et al., 2007; Anand et al., 2008) also supports our view (Fig. 5).

The $\delta^{18}O_w$ record from core SK-17 (Anand et al., 2008) shows depleted values, indicating higher influx of fresh water from the Western Ghats caused by high SWM rainfall, during the B/A (Fig. 6c). The AAS9/21 record (Govil and Naidu, 2010) shows decreased sea surface salinity during the B/A caused by increased fresh water flux into the eastern Arabian Sea that was derived from SWM rainfall (Fig. 6d). The positive correlation between Somali upwelling (high biogenic silica fluxes and lower SSTs) and SWM rainfall in the Western Ghats (high fresh water influx to the eastern Arabian Sea) during the B/A contrasts with the present-day scenario as observed by Vecchi and Harrison (2004). Presently, the moisture source for SWM rainfall is the Arabian Sea and the central Indian Ocean (IOWP), which is affected by SWM upwelling (Izumo et al., 2008). If the central Indian Ocean were the only source of moisture for SWM rainfall during the B/A, then the observed co-variation is possible. Thus, it is proposed that the moisture source for SWM rainfall during the B/A period was different from the modern source. The other possibility, that rainfall in south-western India was enhanced due to a strong NE monsoon during the B/A, is unlikely because the siliceous productivity in the western Arabian Sea related to the NE monsoon has not been reported (Koning et al., 1997; Ramaswamy and Gaye, 2006). In contrast to the B/A, the upwelling in the western Arabian Sea was weak during the YD, as revealed by the low biogenic silica fluxes and high SSTs (Huguet et al., 2006). Furthermore, the high $\delta^{18}O_w$ and high surface salinity values in the eastern Arabian Sea (Anand et al., 2008; Govil and Naidu, 2010), which were caused by low freshwater influx, also points to weak SWM rainfall.

4.2.3 Holocene (11–0 ka BP)

The onset of the Holocene is marked by an abrupt increase in biogenic silica flux (Fig. 6a). This sudden increase in biogenic silica fluxes between 11 ka and 9 ka BP might have been caused by the intensification of the SWM (extended season) due to a northward shift of the ITCZ following the peak in Northern Hemisphere solar insolation (Fleitmann et al., 2007). Somali basin SST records (Saher et al., 2007; Huguet et al., 2006; Anand et al., 2008) also shows a pronounced decrease at the onset of the Holocene, but not up to the levels seen during the B/A. The $\delta^{18}O_w$ and salinity records (Anand et al., 2008; Govil and Naidu, 2010) display values similar to those of the YD during the early Holocene (Fig. 6c and 6d), indicating reduced rainfall (lower fresh water influx) over the Western Ghats. This negative correlation between Somali upwelling and SWM rainfall over south-western India during the early Holocene (11 ka to 9 ka BP), marks the establishment of the modern-day climate system. The increased Somali upwelling in the western Arabian Sea during the early Holocene reduced the IOWP expanse during the SWM, thereby resulting in lower rainfall over the Western Ghats. Upwelling strength decreased after 9 ka BP (Fig. 6a) in the western Arabian Sea compared to the early Holocene but persisted above YD and B/A levels, indicating the presence of the SWM with reduced wind strengths relative to the early Holocene. This reduction in upwelling at 9 ka BP allowed the westward extension of the IOWP during the SWM that increased both, moisture availability over the Arabian Sea and rainfall over the

Clim. Past Discuss., https://doi.org/10.5194/cp-2017-77
Manuscript under review for journal Clim. Past
Discussion started: 7 July 2017

Western Ghats. The SK-17 and AAS9/21 records show decreases in the $\delta^{18}O$ of surface water and surface salinity, respectively, after 9 ka BP, pointing towards an increase in fresh water influx from the Western Ghats at this time (Anand et al., 2008; Govil and Naidu, 2010). During the last 8 ka, along with the gradually increasing upwelling trend, there are two events showing enhanced upwelling centered on 5 and 2 ka BP, marked by slight increases in biogenic silica fluxes in our record from core 4018 and decreases in Somali basin SSTs (Huguet et al., 2006; Saher et al., 2007; Anand et al., 2008). However, the SK-17 record (Anand et al., 2008) shows slight increases in the $\delta^{18}O_w$ of surface waters during the last 8 ka (Fig. 6c). The asynchronous short variations may be due to dissimilarities in sampling intervals and chronology. The core AAS9/21 (Govil and Naidu, 2010) shows low salinity values for the last 8 ka BP, with a noticeable period of low salinity between 5 and 3 ka BP. The low biogenic silica fluxes observed in our core during the same time period (5 to 3 ka BP) indicate lower upwelling but more rainfall during the SWM (reflecting a wider IOWP). The speleothem record from Oman (Fleitmann et al., 2007) also exhibits anti-correlation with the Somali upwelling record (Fig. 6b), indicating the influence of Somali upwelling on rainfall over the Arabian Peninsula during the SWM.

Overall, it has been noted that the Somali upwelling had a negative impact on southwest monsoon rainfall over south-western India throughout the Holocene. This finding becomes more alarming in context of the modelling study by deCastro et al. (2016) which shows that the Somali upwelling would increase during the twenty-first century.

5 Conclusions

The present study demonstrates the use of biogenic silica fluxes as a proxy for the temporal variations in the strength of the Somali upwelling during the last 18.5 ka. Some of the salient findings of the present study are summarized below:

1. The Somali upwelling was weak during the LGP coeval with the weak southwest monsoon.
2. The post-glacial onset of the southwest monsoon was marked by an increase in the strength of the Somali upwelling at 15 ka BP, with eastern Arabian Sea records showing increased southwest monsoon rainfall.
3. The Somali upwelling was weak between 13 and 11 ka BP, indicating another phase of weak southwest monsoon similar to that of the LGP. Overall, records of the Somali upwelling and southwest monsoon rainfall exhibit positive correlations between 18.5 and 11 ka BP.
4. A change in correlation from positive to negative between the strength of the Somali upwelling and southwest monsoon rainfall occurred at 11 ka BP at the beginning of the Holocene, which marks the establishment of modern day climate system.
5. Enhanced Somali upwelling during the last 11 ka BP, except for the decline at 8 ka BP, had a negative impact on southwest monsoon rainfall.
6. Both, latitudinal shifts in the Intertropical Convergence Zone (ITCZ) and changes in moisture source regions act as causative factors for the reversal in the relationship between upwelling and southwest monsoon rainfall.

7. Future observational and modelling studies on southwest monsoon rainfall reconstruction and prediction should incorporate variations in the moisture source region.

Acknowledgments

Balaji D. is thankful to the Council of Scientific and Industrial Research (CSIR) of India for providing support through a CSIR-NET-Senior Research Fellowship. Ravi Bhushan thanks the Director of the PRL for research grant support. We thank Dr. Alpa Sridhar for critical comments and suggestions on the manuscript.

References

Anand, P., Kroon, D., Singh, A. D., Ganeshram, R. S., Ganssen, G., and Elderfield, H.: Coupled sea surface temperature–seawater $\delta^{18}O$ reconstructions in the Arabian Sea at the millennial scale for the last 35 ka, Paleoceanography, 23, 2008.

Annamalai, H., and Liu, P.: Response of the Asian summer monsoon to changes in El Nino properties, Quarterly Journal of the Royal Meteorological Society, 131, 805-831, 2005.

Beal, L. M., and Chereskin, T. K.: The volume transport of the Somali Current during the 1995 southwest monsoon, Deep Sea Research Part II: Topical Studies in Oceanography, 50, 2077-2089, 2003.

Berrisford, P., Kållberg, P., Kobayashi, S., Dee, D., Uppala, S., Simmons, A., Poli, P., and Sato, H.: Atmospheric conservation properties in ERA-Interim, Quarterly Journal of the Royal Meteorological Society, 137, 1381-1399, 2011.

Burckle, L. H.: Distribution of diatoms in sediments of the northern Indian Ocean: Relationship to physical oceanography, Marine Micropaleontology, 15, 53-65, 1989.

Carter, S. J., and Colman, S. M.: Biogenic silica in Lake Baikal sediments: results from 1990–1992 American cores, Journal of Great Lakes Research, 20, 751-760, 1994.

Clemens, S. C., Prell, W. L., and Howard, W. R.: Retrospective dry bulk density estimates from southeast Indian Ocean sediments—comparison of water loss and chloride-ion methods, Marine geology, 76, 57-69, 1987.

Dahl, K. A., and Oppo, D. W.: Sea surface temperature pattern reconstructions in the Arabian Sea, Paleoceanography, 21, 2006.

Findlater, J.: Observational aspects of the low-level cross-equatorial jet stream of the western Indian Ocean, in: Monsoon Dynamics, Springer, 1251-1262, 1978.

Fleitmann, D., Burns, S. J., Mangini, A., Mudelsee, M., Kramers, J., Villa, I., Neff, U., Al-Subbary, A. A., Buettner, A., and Hippler, D.: Holocene ITCZ and Indian monsoon dynamics recorded in stalagmites from Oman and Yemen (Socotra), Quaternary Science Reviews, 26, 170-188, 2007.

Goswami, B., Krishnamurthy, V., and Annmalai, H.: A broad-scale circulation index for the interannual variability of the Indian summer monsoon, Quarterly Journal of the Royal Meteorological Society, 125, 611-633, 1999.

Goswami, B., Madhusoodanan, M., Neema, C., and Sengupta, D.: A physical mechanism for North Atlantic SST influence on the Indian summer monsoon, Geophysical Research Letters, 33, 2006.

Govil, P., and Naidu, P. D.: Evaporation-precipitation changes in the eastern Arabian Sea for the last 68 ka: Implications on monsoon variability, Paleoceanography, 25, 2010.

Gupta, A. K., Anderson, D. M., and Overpeck, J. T.: Abrupt changes in the Asian southwest monsoon during the Holocene and their links to the North Atlantic Ocean, Nature, 421, 354-357, 2003.

Haake, B., Ittekkot, V., Rixen, T., Ramaswamy, V., Nair, R., and Curry, W.: Seasonality and interannual variability of particle fluxes to the deep Arabian Sea, Deep Sea Research Part I: Oceanographic Research Papers, 40, 1323-1344, 1993.

Hahn, D. G., and Shukla, J.: An apparent relationship between Eurasian snow cover and Indian monsoon rainfall, Journal of the Atmospheric Sciences, 33, 2461-2462, 1976.

Huguet, C., Kim, J. H., Sinninghe Damsté, J. S., and Schouten, S.: Reconstruction of sea surface temperature variations in the Arabian Sea over the last 23 kyr using organic proxies (TEX86 and U37K′), Paleoceanography, 21, 2006.

Hurd, D. C.: Interactions of biogenic opal, sediment and seawater in the Central Equatorial Pacific, Geochimica et cosmochimica acta, 37, 2257IN12267-22662282, 1973.

Isaji, Y., Kawahata, H., Ohkouchi, N., Ogawa, N. O., Murayama, M., Inoue, K., and Tamaki, K.: Varying responses to Indian monsoons during the past 220 kyr recorded in deep-sea sediments in inner and outer regions of the Gulf of Aden, Journal of Geophysical Research: Oceans, 120, 7253-7270, 2015.

Ivanochko, T. S., Ganeshram, R. S., Brummer, G.-J. A., Ganssen, G., Jung, S. J., Moreton, S. G., and Kroon, D.: Variations in tropical convection as an amplifier of global climate change at the millennial scale, Earth and Planetary Science Letters, 235, 302-314, 2005.

Izumo, T., Montégut, C. B., Luo, J.-J., Behera, S. K., Masson, S., and Yamagata, T.: The role of the western Arabian Sea upwelling in Indian monsoon rainfall variability, Journal of Climate, 21, 5603-5623, 2008.

Koning, E., Brummer, G.-J., Van Raaphorst, W., Van Bennekom, J., Helder, W., and Van Iperen, J.: Settling, dissolution and burial of biogenic silica in the sediments off Somalia (northwestern Indian Ocean), Deep Sea Research Part II: Topical Studies in Oceanography, 44, 1341-1360, 1997.

Koning, E., Van Iperen, J., Van Raaphorst, W., Helder, W., Brummer, G.-J., and Van Weering, T.: Selective preservation of upwelling-indicating diatoms in sediments off Somalia, NW Indian Ocean, Deep Sea Research Part I: Oceanographic Research Papers, 48, 2473-2495, 2001.

Krishnamurthy, L., and Krishnamurthy, V.: Teleconnections of Indian monsoon rainfall with AMO and Atlantic tripole, Climate Dynamics, 46, 2269-2285, 2016.

Krishnan, R., and Sugi, M.: Pacific decadal oscillation and variability of the Indian summer monsoon rainfall, Climate Dynamics, 21, 233-242, 2003.

M., d., Sousa, M., Santos, F., Dias, J., and Gómez-Gesteira, M.: How will Somali coastal upwelling evolve under future warming scenarios?, Scientific Reports, 6, 2016.

Mooley, D., Parthasarathy, B., and Pant, G.: Relationship between Indian Summer Monsoon Rainfall and Location of the Ridge at the 500-mb Level along 75° E, Journal of climate and applied meteorology, 25, 633-640, 1986.

Mortlock, R. A., and Froelich, P. N.: A simple method for the rapid determination of biogenic opal in pelagic marine sediments, Deep Sea Research Part A. Oceanographic Research Papers, 36, 1415-1426, 1989.

Naidu, P. D., and Malmgren, B. A.: A high-resolution record of late Quaternary upwelling along the Oman Margin, Arabian Sea based on planktonic foraminifera, Paleoceanography, 11, 129-140, 1996.

Ninomiya, K., and Kobayashi, C.: Precipitation and Moisture Balance of the Asian Summer Monsoon in 1991, Journal of the Meteorological Society of Japan. Ser. II, 77, 77-99, 1999.

Pant, G. B., and Kumar, K. R.: Climates of south Asia, John Wiley & Sons, 1997.

Parthasarathy, B., Diaz, H., and Eischeid, J.: Prediction of all-India summer monsoon rainfall with regional and large-scale parameters, Journal of Geophysical Research: Atmospheres, 93, 5341-5350, 1988.

Parthasarathy, B., Kumar, K. R., and Munot, A.: Evidence of secular variations in Indian monsoon rainfall–circulation relationships, Journal of Climate, 4, 927-938, 1991.

Qasim, S.: Biological productivity of the Indian Ocean, Indian Journal of Marine Sciences, 6, 16, 1977.

R., S.: Ocean Data View, 2016.

Ramaswamy, V., and Gaye, B.: Regional variations in the fluxes of foraminifera carbonate, coccolithophorid carbonate and biogenic opal in the northern Indian Ocean, Deep Sea Research Part I: Oceanographic Research Papers, 53, 271-293, 2006.

Saher, M., Jung, S., Elderfield, H., Greaves, M., and Kroon, D.: Sea surface temperatures of the western Arabian Sea during the last deglaciation, Paleoceanography, 22, 2007.

Schott, F., Swallow, J. C., and Fieux, M.: The Somali Current at the equator: annual cycle of currents and transports in the upper 1000 m and connection to neighbouring latitudes, Deep Sea Research Part A. Oceanographic Research Papers, 37, 1825-1848, 1990.

Schott, F. A., Xie, S. P., and McCreary, J. P.: Indian Ocean circulation and climate variability, Reviews of Geophysics, 47, 2009.

Sirocko, F., and Lange, H.: Clay-mineral accumulation rates in the Arabian Sea during the late Quaternary, Marine Geology, 97, 105-119, 1991.

Sirocko, F., Sarnthein, M., Lange, H., and Erlenkeuser, H.: Atmospheric summer circulation and coastal upwelling in the Arabian Sea during the Holocene and the last glaciation, Quaternary Research, 36, 72-93, 1991.

Sirocko, F., Sarnthein, M., Erlenkeuser, H., Lange, H., Arnold, M., and Duplessy, J.: Century-scale events in monsoonal climate over the past 24,000 years, Nature, 364, 322-324, 1993.

Sirocko, F., Garbe-Schönberg, D., and Devey, C.: Processes controlling trace element geochemistry of Arabian Sea sediments during the last 25,000 years, Global and Planetary Change, 26, 217-303, 2000.

Tiwari, M., Ramesh, R., Bhushan, R., Sheshshayee, M. S., Somayajulu, B. L., Jull, A., and Burr, G. S.: Did the Indo-Asian summer monsoon decrease during the Holocene following insolation?, Journal of Quaternary Science, 25, 1179-1188, 2010.

Vecchi, G. A., and Harrison, D.: Interannual Indian rainfall variability and Indian Ocean sea surface temperature anomalies.. In Earth Climate: The Ocean-Atmosphere Interaction, C. Wang, S. P. Xie & J.A. Carton (eds.), American Geophysical Union., Geophysical Monograph, 147, 247-259, 2004.

Wyrtki, K.: Physical oceanography of the Indian Ocean, in: The biology of the Indian Ocean, Springer, 18-36, 1973.

Yadav, R. K.: On the relationship between east equatorial Atlantic SST and ISM through Eurasian wave, Climate Dynamics, 48, 281-295, 2017.

Young, D. K., and Kindle, J. C.: Physical processes affecting availability of dissolved silicate for diatom production in the Arabian Sea, Journal of Geophysical Research: Oceans, 99, 22619-22632, 1994.

Clim. Past Discuss., https://doi.org/10.5194/cp-2017-77
Manuscript under review for journal Clim. Past
Discussion started: 7 July 2017

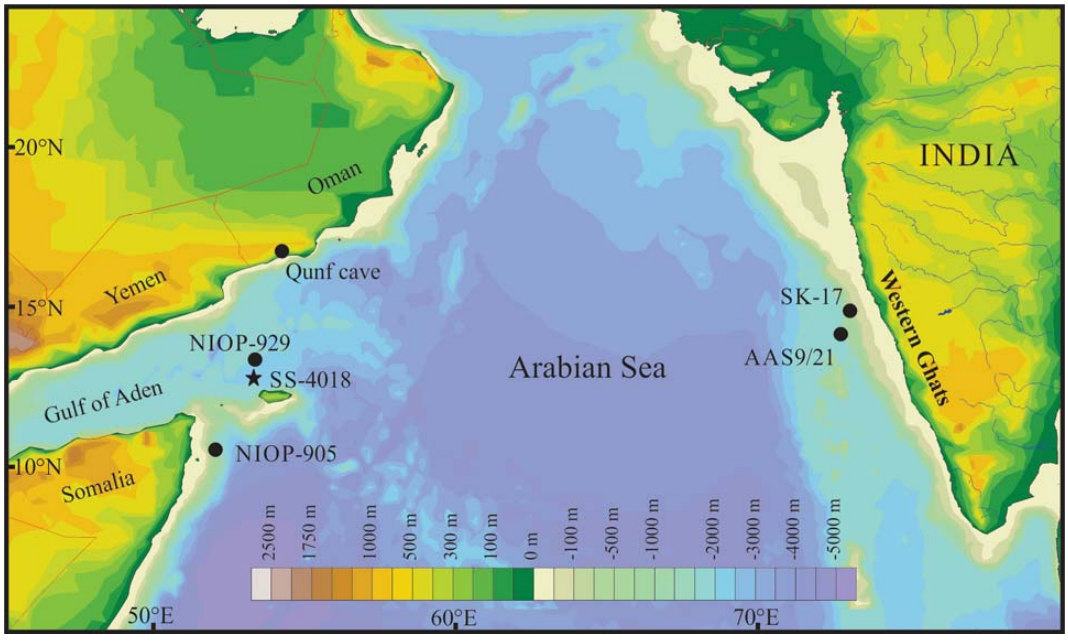

Figure 1: Location of sediment core SS-4018 (filled star) in the Arabian Sea. Also shown are the sites discussed in the paper: NIOP-929 (Saher et al., 2007), NIOP-905 (Huguet et al., 2006), SK-17 (Anand et al., 2008), Qunf cave (Fleitmann et al., 2007), AAS9/21 (Govil and Naidu, 2010).

Clim. Past Discuss., https://doi.org/10.5194/cp-2017-77
Manuscript under review for journal Clim. Past
Discussion started: 7 July 2017

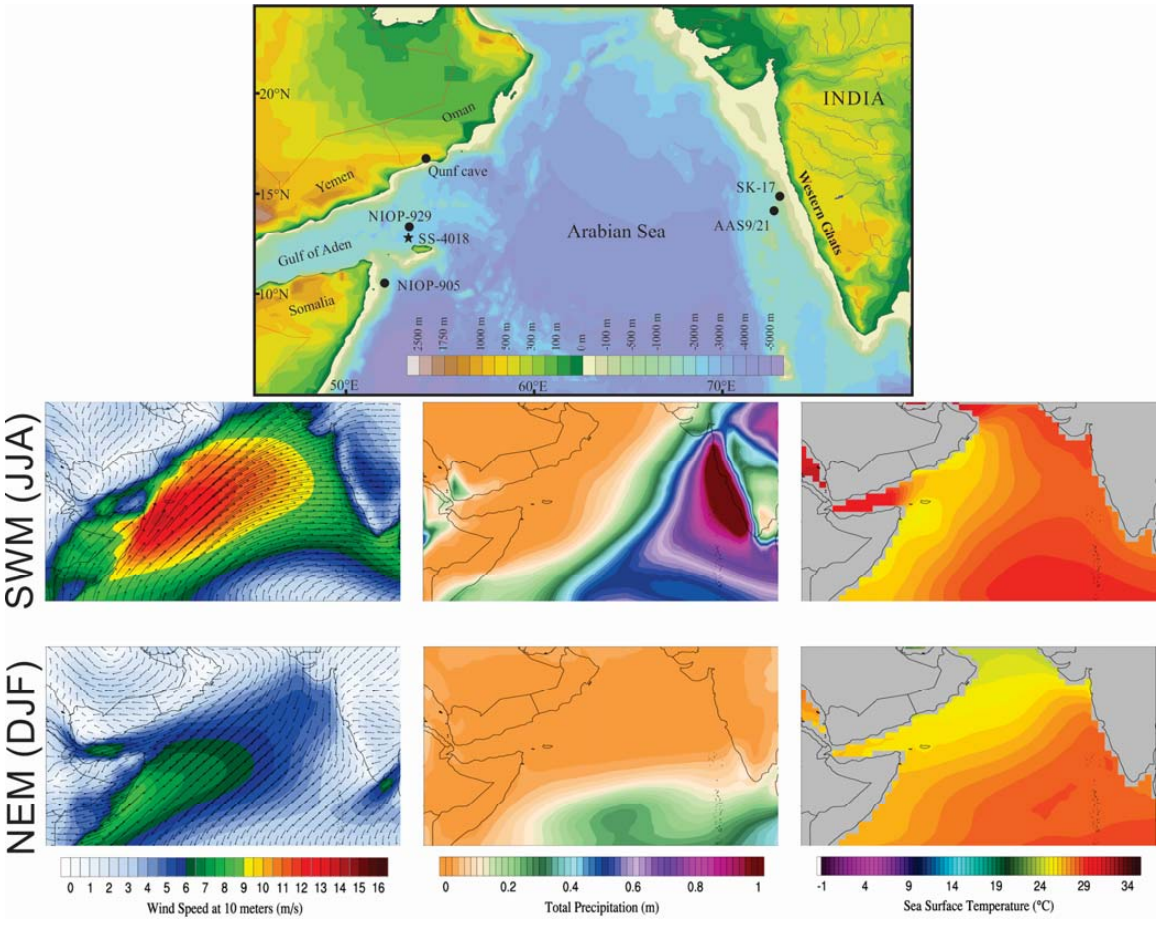

375 **Figure 2: Location of our sediment core SS4018 in the western Arabian Sea. Also shown are the sites discussed in the manuscript. Bottom figures shows the seasonal changes in Wind speed, Precipitation and SST during southwest (SWM) and northeast monsoon (NEM). ECMWF-ERA-Interim data (Berrisford et al., 2011) used and the image obtained using Climate Reanalyzer (http://cci-reanalyzer.org), Climate Change Institute, University of Maine, USA.**

Clim. Past Discuss., https://doi.org/10.5194/cp-2017-77
Manuscript under review for journal Clim. Past
Discussion started: 7 July 2017

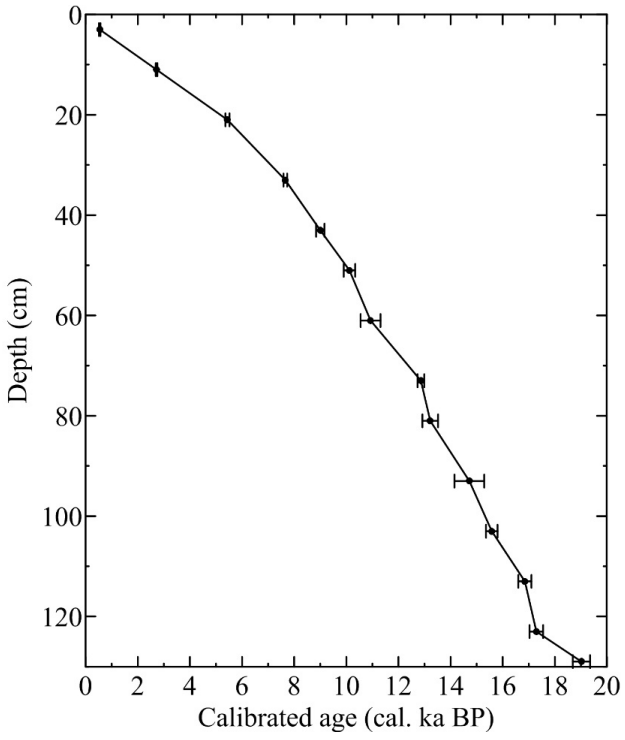

Figure 3: Age depth model of the sediment core SS-4018 (adopted from Tiwari et al., 2010). The error bars marks one sigma uncertainty in calibrated age.

Clim. Past Discuss., https://doi.org/10.5194/cp-2017-77
Manuscript under review for journal Clim. Past
Discussion started: 7 July 2017

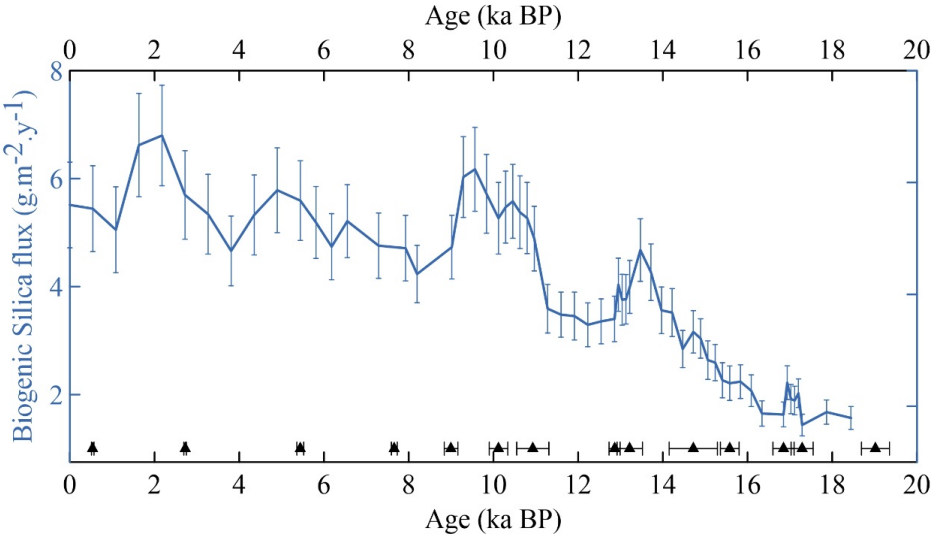

Figure 4: Temporal variation of Biogenic silica flux with two sigma uncertainty in sediment core SS4018. Filled triangles at the bottom of the plot marks the age-control points with one sigma uncertainity.

Clim. Past Discuss., https://doi.org/10.5194/cp-2017-77
Manuscript under review for journal Clim. Past
Discussion started: 7 July 2017

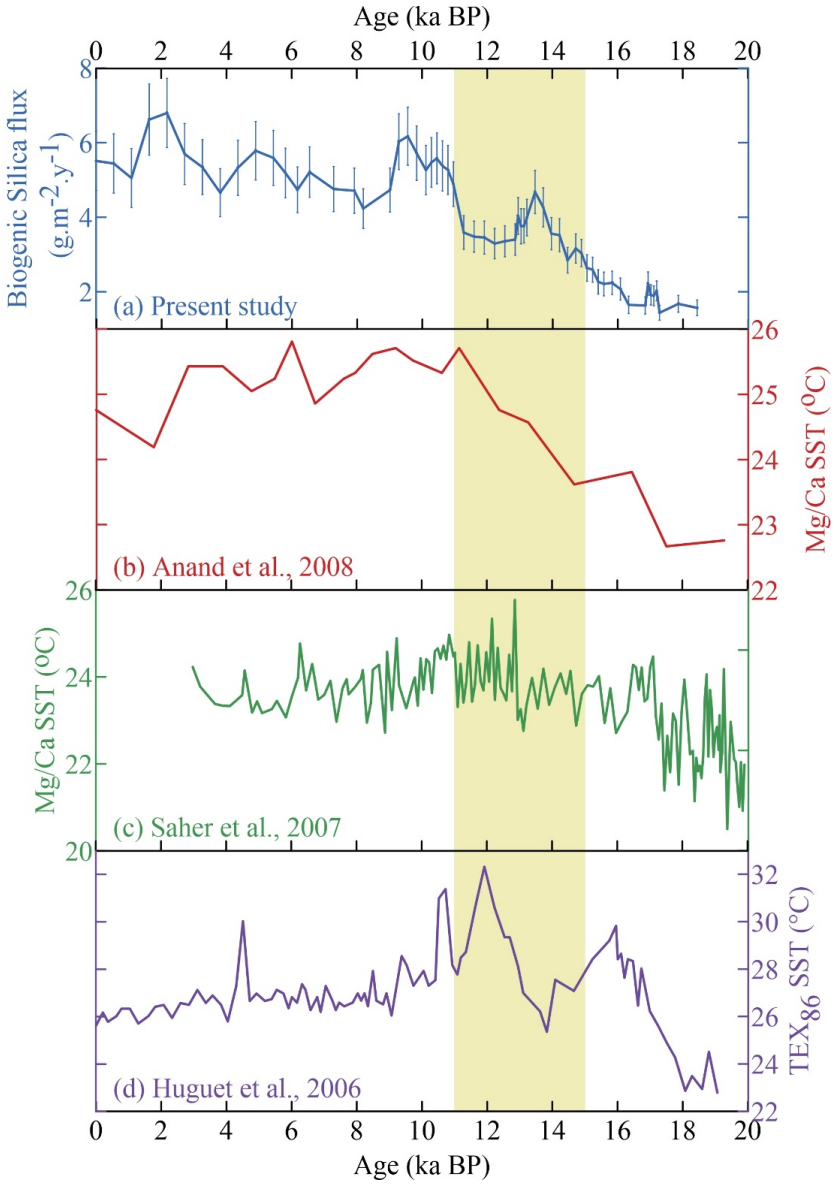

Figure 5: Comparison of Somali upwelling with western Arabian Sea SST records. a) Biogenic silica flux, b) Mg/Ca based SST from NIOP-905 core (Anand et al., 2008), c) Mg/Ca based SST from NIOP-929 core (Saher et al., 2007), d) TEX86 SST from NIOP-905 core (Huguet et al., 2006). Shaded region marks the Deglacial Period (DP).

Clim. Past Discuss., https://doi.org/10.5194/cp-2017-77
Manuscript under review for journal Clim. Past
Discussion started: 7 July 2017

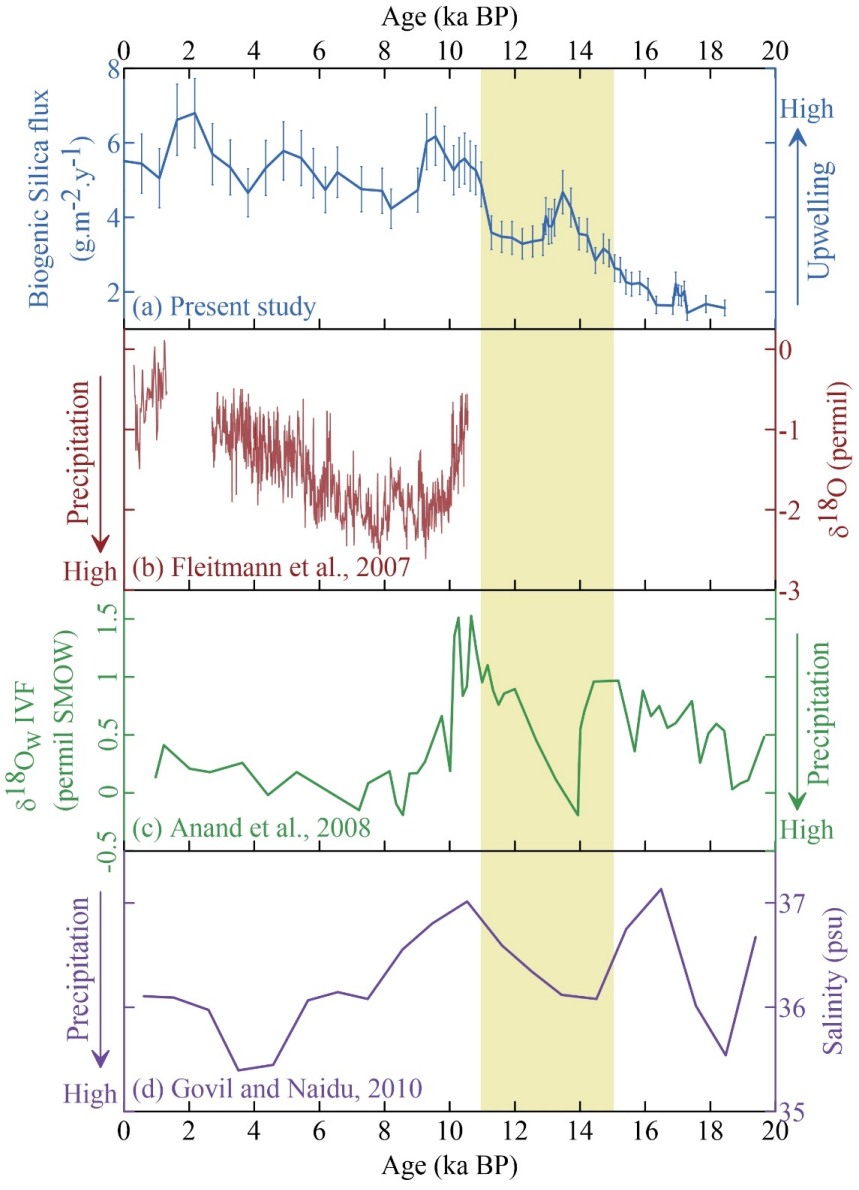

390

Figure 6: Comparison of Somali upwelling with southwest monsoon rainfall records. (a) Biogenic silica flux (present study), (b) Oman speleothem record, (c) $\delta^{18}O_w$ data from sediment core SK-17, (d) Salinity record of sediment core AAS9/21. Shaded region marks the Deglacial Period (DP).

Clim. Past Discuss., https://doi.org/10.5194/cp-2017-77
Manuscript under review for journal Clim. Past
Discussion started: 7 July 2017

Climate of the Past Discussions

Age (ky)	B. Si (%)	σ B.Si	B.Si flux (g/m^2/y)	σ B.Si flux	Age (ky)	B. Si (%)	σ B.Si	B.Si flux (g/m^2/y)	σ B.Si flux
0.00	12.58	0.22	5.51	0.79	12.23	6.41	0.11	3.29	0.41
0.54	12.58	0.25	5.44	0.80	12.54	6.49	0.16	3.36	0.42
1.09	12.58	0.28	5.05	0.80	12.86	6.49	0.20	3.40	0.42
1.63	15.20	0.20	6.62	0.96	12.95	7.76	0.13	4.03	0.49
2.17	14.81	0.14	6.80	0.93	13.04	7.37	0.18	3.76	0.47
2.72	13.06	0.05	5.70	0.82	13.13	7.24	0.09	3.77	0.46
3.26	11.70	0.21	5.34	0.74	13.22	7.74	0.13	3.99	0.49
3.81	10.23	0.17	4.66	0.65	13.47	9.06	0.21	4.68	0.58
4.35	11.79	0.10	5.33	0.74	13.72	8.23	0.16	4.27	0.52
4.90	12.49	0.13	5.78	0.79	13.97	6.83	0.11	3.56	0.43
5.44	11.64	0.22	5.59	0.74	14.22	6.83	0.22	3.52	0.44
5.81	10.52	0.17	5.19	0.67	14.47	5.41	0.10	2.84	0.34
6.18	9.74	0.04	4.74	0.61	14.72	6.11	0.16	3.16	0.39
6.55	10.52	0.29	5.21	0.68	14.89	5.74	0.09	3.04	0.36
7.29	9.59	0.12	4.76	0.61	15.06	5.49	0.19	2.64	0.36
7.93	9.59	0.15	4.71	0.61	15.24	5.24	0.14	2.59	0.34
8.20	8.31	0.19	4.23	0.53	15.41	5.07	0.15	2.27	0.32
9.02	9.35	0.10	4.73	0.59	15.58	5.08	0.04	2.21	0.32
9.29	11.88	0.09	6.03	0.75	15.83	4.94	0.08	2.24	0.31
9.56	12.28	0.19	6.17	0.78	16.09	4.53	0.17	2.07	0.29
9.84	11.57	0.14	5.72	0.73	16.34	3.66	0.11	1.65	0.23
10.12	10.43	0.21	5.26	0.66	16.85	3.54	0.13	1.63	0.23
10.29	10.57	0.10	5.47	0.67	16.94	4.75	0.20	2.22	0.31
10.46	10.82	0.14	5.58	0.68	17.03	4.17	0.15	1.92	0.27
10.63	10.59	0.20	5.38	0.67	17.11	4.04	0.17	1.89	0.27
10.80	10.45	0.11	5.27	0.66	17.20	4.17	0.08	2.02	0.26
10.97	9.47	0.12	4.89	0.60	17.29	3.05	0.12	1.44	0.20
11.28	7.04	0.17	3.59	0.45	17.87	3.52	0.09	1.68	0.22
11.60	6.59	0.09	3.48	0.42	18.44	3.25	0.11	1.57	0.21
11.91	6.92	0.17	3.45	0.44					

Table 1: Biogenic silica concentration and flux data.